Correlation of volatile products from fast cellulose pyrolysis

ARTICLE *in* INDUSTRIAL & ENGINEERING CHEMISTRY PROCESS DESIGN AND DEVELOPMENT · JANUARY 1986

DOI: 10.1021/i200032a027

Correlation of Volatile Products from Fast Cellulose Pyrolysis

Toshitaka Funazukuri

Department of Chemical Engineering, Yokohama National University, Yokohama, Japan

Robert R. Hudgins and Peter L. Silveston*

Department of Chemical Engineering, University of Waterloo, Waterloo, Ontario, Canada N2L 3G1

The weight loss and the product yields from cellulose powder, cellulose particles, and filter paper were measured simultaneously under flash pyrolysis conditions. Products can be grouped into two distinct types. One is a CO behavior for which yields increase with the weight loss and at weight loss above 40% also become a function of pyrolysis temperature. The second is a CO_2 behavior for which yields are proportional to the weight loss and independent of pyrolysis temperature. Yields of both the CO behavior and CO_2 behavior products correlate linearly in log–log plots with the CO yields and with CO_2 yields, respectively. Because CO yields correlate well with the weight loss and pyrolysis temperature, major gaseous and liquid products obtained from flash pyrolysis of cellulose powder or particles can be predicted accurately. Variables such as heating rate, particle size, and pyrolysis temperature do not affect the relationships.

Short contact time or flash pyrolysis is one of the alternatives under consideration for the conversion of biomass into liquid or gaseous fuel or perhaps into chemical feedstocks. A variety of compounds are formed in flash pyrolysis so that it would be desirable to be able to predict yields of at least the major products as a function of the pyrolysis device and operating conditions such as heating rate of the biomass, final temperature, particle size, and gas-phase composition. Our objective in this paper is to contribute toward this goal.

The approach pursued in our work assumed that the component in the biomass, e.g., cellulose, is the dominant factor in the product distribution. Molecular weight of the component, how it is incorporated in the cell structure of the biomass source or the density of the paper, and the presence of other materials (ash and lignin) were considered to be secondary factors. This paper considers the pyrolysis of microcrystalline cellulose powder (MCP) with respect to the influence of the flash pyrolysis device, heating rate, final temperature, atmosphere, and particle size on the product distribution.

Summary of the Literature

Compared with the vast literature on slow pyrolysis of cellulose (see, for example: Brunner and Roberts, 1980; Shafizadeh and Bradbury, 1979; Antal et al., 1980; Min, 1977), the literature on flash pyrolysis is very small.

A few studies have been made using a Pyroprobe or a Curie point pyrolyzer (Iglauer and Bentley, 1974; Ohnishi et al., 1975; Hileman et al., 1976) and a fluidized bed (Barooah and Long, 1976; Maa and Bailie, 1978; Scott and Piskorz, 1981a,b). Irradiation was used by Martin (1965) and Shivadev and Emmons (1974) as a heat source. Lewellen et al. (1977) and Hajaligol et al. (1982) pyrolyzed filter paper suspended between two massive electrodes. Unfortunately, weight loss measurement and analysis of volatile products have rarely been carried out simultaneously. Identification of volatile products usually has come from investigations where the pyrolysis reactions went nearly to completion. In such cases, the product distribution could result not only from cellulose pyrolysis but also from secondary cracking and perhaps even char gasification.

Many attempts to identify volatile or tarry components produced from cellulose pyrolysis have been made. We summarize only those carried out on cellulose at relatively high heating rates in Tables I (volatile products) and II (tar). Of these, only in the studies of Martin (1965) and Hajaligol et al. (1982) were all the major pyrolysis products measured. Table II, however, shows that these investigators did not analyze the tar produced. Except for Ohnishi et al. (1975), researchers have employed samples collected at rather slow heating rates. Ohnishi et al., furthermore, carried out just qualitative analysis. A problem with slow heating is that levoglucosan appears to be produced in the initial chain scissions (Berkowitz-Mattuck and Noguchi, 1963; Glassner and Pierce, 1965; Schwenker and Beck, 1963; Wodley, 1971). This product may also be pyrolyzed, so levoglucosan yields and indeed the tar composition should depend significantly upon heating rate.

Studies at slow heating rates indicate that sample size influences pyrolysis kinetics. It would seem that size would also influence the kinetics or product distribution in flash pyrolysis, but up to now, this variable has not been examined. The effect on gas composition, specifically of oxygen, also has not been considered under flash pyrolysis conditions for cellulose. There is evidence from slow heating rate studies that vacuum increases tar yields (Broido, 1966; Shafizadeh and Fu, 1973; Shafizadeh et al., 1979a). Oxygen appears to influence rate (Fairbridge et al., 1978; Kato and Takahashi, 1967) and product distribution at pyrolysis below 300 °C (Shafizadeh and Bradbury, 1979). However, this influence may disappear above that temperature (Sakuma et al., 1981; Schwenker and Beck, 1963; Shafizadeh and Bradbury, 1979).

The influence of heating rate and to a lesser extent of temperature on pyrolysis rates and product distribution has been considered for the flash pyrolysis of cellulose. Several investigators have found an appreciable shift in product distribution from char to greater amounts of gas as the heating rate increases (Kaiser and Friedman, 1968;

* To whom correspondence should be addressed.

0196-4305/86/1125-0172$01.50/0

Table I. Experimental Conditions in Previous Studies on Volatile Products from Cellulose Pyrolysis with Measurements Performed

reference	sample	temp, °C	heating time	atmosphere	CO, CO_2, and H_2O	volatile products	tar	wt loss or char
Berkowitz-Nattuck and Noguchi, 1963	cotton poplin	?	0.5–2 s	helium (1 atm)	**[b]	**	*	
Schwenker and Beck, 1963	cotton yarn	450	10–12 s	air and N_2 (1 atm)	*[a]	*		
Martin, 1965	α-cellulose	transient heating up to 650	0.4–8 s	air (1 atm)	**	**	**	**
Kato, 1967	microcrystalline cellulose	250, 350, and 500	1–5 min	helium (1 atm)		*a[c]		
Kato and Komorita, 1968	tobacco cellulose, microcrystalline cellulose	240–500	2 s to 4 min	helium (1 atm)		**		**
Ohnishi et al., 1975	microcrystalline cellulose	460	5 s	helium (1 atm)			*	
Garn and Denson, 1977a–c	cellulose	430	5 min	helium (1 atm)	*	**		
Sakuma et al., 1981	filter paper	400–800	30 s	nitrogen and air (1 atm)		**	**	**
Hajaligol et al., 1982	filter paper	300–1100	0–30 s	helium (5 psi)	**	**	**	**

[a] * = qualitative measurement. [b] ** = quantitative measurement. [c] *a = semiquantitative measurement.

Lewellen et al., 1977; Maa and Bailie, 1978; Rensfelt et al., 1978). Lewellen et al. (1977) observed no char when heating rates of 10 000 °C/s were used. Hajaligol et al. (1982) observed that the total conversion of sample to volatiles increased as the heating rate decreased at the same temperature. Shafizadeh (1968) concluded that the pyrolysis temperature greatly affects not only the rate of pyrolysis/gasification of cellulose but also the distribution of products. However, he used data obtained at slow heating rates to support his conclusion.

Pyrolysis Systems and Analytical Techniques

Flash pyrolysis was achieved in this study by two devices: a Pyroprobe pyrolyzer and a miniature fluidized bed. Although they operate quite differently, both reactors provide a high heating rate and a short contact time. The latter is achieved by an extremely rapid rise in temperature of the heating coil in the Pyroprobe and a short residence time in the fluidized bed. Essentially, any operating temperature can be used in either device.

Pyroprobe Pyrolyzer. The "Pyroprobe" 100 Solid Pyrolyzer, manufactured by Chemical Data Systems, is shown schematically in Figure 1. The heating element inserted into the probe body is a 0.36-mm platinum wire formed into a coil 15 mm in length by 3 mm in diameter. Cellulose samples were held in 1.5 mm by 2.5 cm quartz boats which were placed in roughly the center of the coil. The probe was attached to a gas chromatograph by means of an interface block. Helium carrier gas circulated through the probe as shown at all times. The instrument has a final temperature setting continuously adjustable from ambient to 1000 °C. Eight nominal heating rates between 0.1 and 20 °C/ms and ten heating intervals ranging from 20 ms to 20 s are available. These intervals include the heating period as well as a final "soaking" period at the final temperature.

By imbedding a microthermocouple in the sample, it was observed that the actual temperatures attained and the heating rates in the sample differed significantly from the nominal values set on the instrument (Funazukuri, 1983). The investigation permitted the real temperatures and heating rates experienced by the samples to be estimated.

The interface connecting the probe to the GC was held at 150 °C. This was set by the use of Viton O-rings and by the slow pyrolysis of the sample prior to ignition if

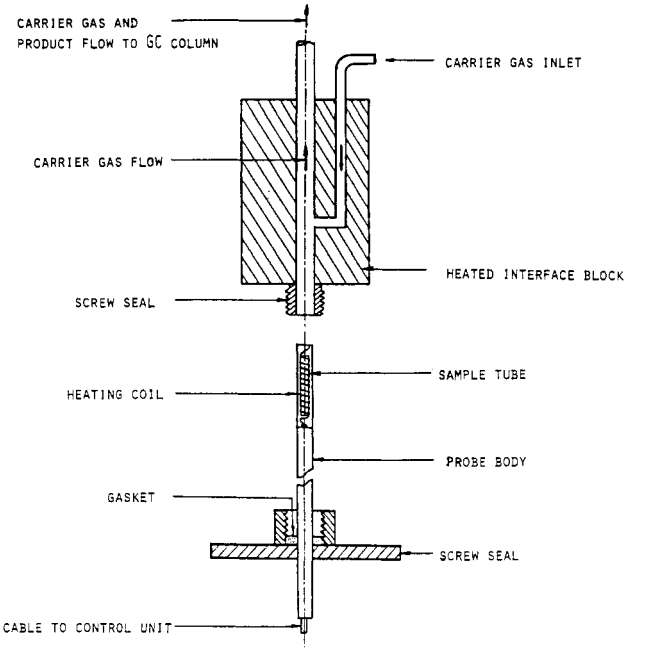

Figure 1. Schematic of the Pyroprobe 100 and its interface to a gas chromatograph.

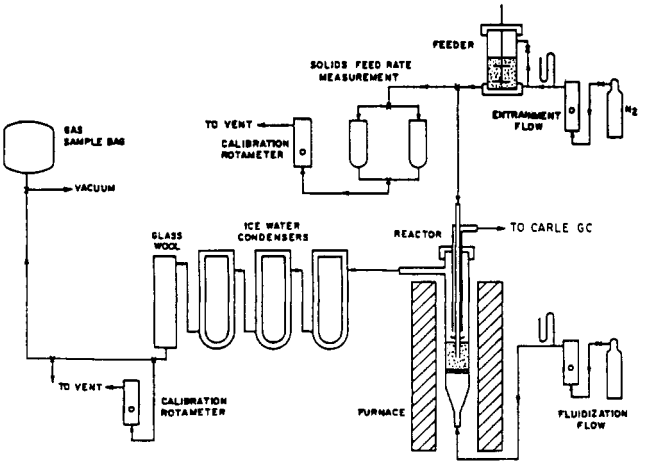

Figure 2. Schematic diagram of the fluidized bed experimental system.

Table II. Experimental Conditions in Previous Studies of Tarry Compounds Produced from Cellulose Pyrolysis with Products Measured

reference	sample	temp, °C	heating time	atmosphere	component A[c]	B[d]	C[e]	D[f]
Broido et al., 1975	cellulose powder	295–335	?	6.7×10^{-3} Pa 0.27 1.17×10^{4}	**[b]		**	
Byrne et al., 1966	cotton	420	6 min	vacuum	**	**		
Tsuchiya and Sumi, 1970	filter paper	320–520	20 min	vacuum	**	**		
Ohnishi et al., 1975	microcrystalline cellulose powder	460	5 s	helium (1 atm)			*[a]	
Shafizadeh et al., 1978	cellulose powder cotton linter	315–390	5–30 min	nitrogen (1.5 and 680 torr)	**	**		*
Shafizadeh et al., 1979a	cellulose powder filter paper microcrystalline cellulose powder cotton fabric	300–500	3–180 min	vacuum nitrogen (1 atm)	**	**		
Shafizadeh et al., 1979b	cellulose powder kraft paper newsprint	275–425	20 min	nitrogen (1.5, 150, and 760 torr)	**		**	**

[a] * = qualitative measurement. [b] ** = quantitative measurement. [c] A = 1,6-anhydro-β-D-glucopyranose (levoglucosan). [d] B = 1,6-anhydro-β-D-glucofuranose. [e] C = 1,6-anhydro-3,4-dideoxy-β-D-glycerohex-3-enopyranos-2-ulose (levoglucosenone). [f] D = 1,4:3,6-dianhydro-α-D-glucopyranose.

higher interface temperatures were employed.

Fluidized Bed. Figure 2 shows the fluidized bed system used in this study. Details of the bed itself are given in Figure 3. The assembly shown in Figure 2 was built by Scott and Piskorz (1981a,b) for the study of the flash pyrolysis of coal and wood.

Pyrolysis occurs in a bed of fluidized sand supported by a porous stainless steel distribution plate. Fluidizing gas is introduced from the bottom through a preheating tube 1 m in length. Both the preheater and fluidized bed were mounted in a three-zone Lindberg electric tube furnace. The preheating tube was long enough to bring the fluidizing gas to bed temperature.

The low rate of cellulose feed needed for the system was achieved by using an entrainment feeder described by Scott and Piskorz (1981a). Cellulose entrained in carrier gas entered the bed through the central, downwardly directed tube in Figure 3. The tip of this tube was immersed in the fluidized sand. The concentric tube, terminating in a 6.3 mm o.d. outlet, served as a sampling line to a Carle GC with a heated sampling loop. This GC periodically sampled the off-gas and was used to ensure the assembly operated at steady state.

The 12.7 mm o.d. outlet seen in Figure 3 was connected to the first of three, water-cooled glass condensers by about 40 cm of Teflon tubing. Almost all the tar formed and the char eluted from the bed was trapped in the condensers or in the connecting tubing. The remaining tar was caught in a glass-wool-filled column. Gas was collected in an inflatable bag.

A run using this equipment lasted about 30 min. Weighing provided the amount of cellulose fed to the fluidized bed and the char caught in the bed. Washing of the glass wool, tubing and condensers with ethanol and weighing the residue after filtration measured the char eluted. The tar yield was obtained by weighing the residue after filtering and evaporating the solvent. GC analysis of the gas bag contents and measurement of the gas volume gave the non-condensable, volatile products produced.

Chromatographic Procedure. With the Pyroprobe, volatile pyrolysis products were carried from the probe directly onto either a 2.4-m 100/120-mesh Porapak Q chromatograph column or a 1.8-m column of 100/120-mesh Porapak T. Both FID and TC detectors were available on the gas chromatograph used. Temperature programming was employed. Figure 4a shows an FID chromatogram obtained with the 2.4-m Porapak Q column. Note the imperfect resolution of acetone and propionaldehyde, acetic acid and isobutyraldehyde, the lower molecular weight ketones, and acrolein and furan. Figure 4b shows the corresponding chromatogram obtained with the Porapak T column. Peaks that could not be separated were methanol and acetaldehyde, acrolein and propionaldehyde, 2-methylfuran and isobutyraldehyde, the ketones, 2,5-dimethylfuran and crotonaldehyde, and toluene and acetic acid. These compounds were measured by using both columns. Some higher molecular weight peaks were not identified.

The gas bag was sampled by using a dual-channel chromatograph equipped with 1.8-m 100/120-mesh Porapak T and 1.8-m 80/100-mesh Porapak Q columns. Both

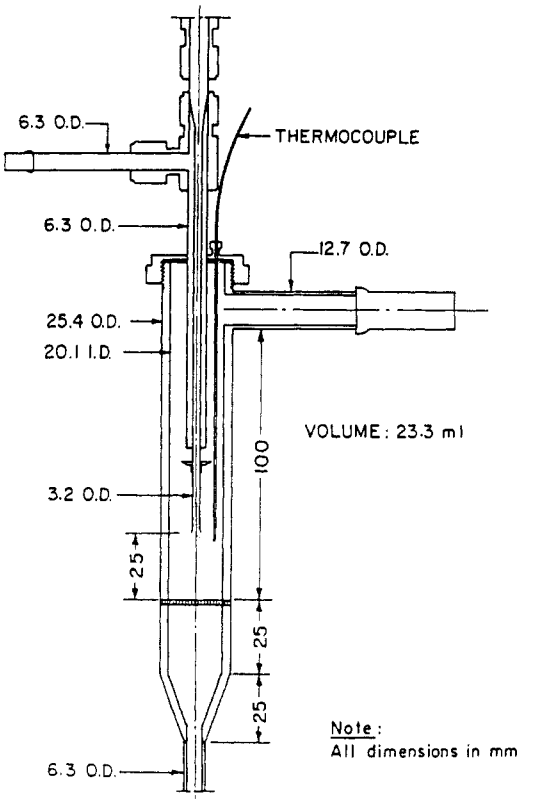

Figure 3. Cross section of the fluidized bed with dimensions.

Table III. Experimental Variables

variables		pyroprobe pyrolyzer	fluidized bed
sample pyrolyzed	sample size		
MCP[a]	0.053–0.074 mm (200/270 mesh)	x	x
cellulose particles	0.43–0.85 mm (20/40 mesh)	x	x
filter paper (Whatman ashless No. 44)	5 × 1 × 0.2 mm strips	x	
heating conditions			
temp, °C		600–1000[b] (400–720)	310–770
heating rate, °C/ms		0.1 and 20[b] (0.035 and 0.3)	?
heating interval/contact time, s		0.5–20	0.46[c]
composition of carrier or fluidization gas			
helium		x	
nitrogen			x
carbon monoxide			x
carbon dioxide			x
hydrogen + nitrogen			x

[a] Microcrystalline cellulose powder. [b] Indicated values on the Pyroprobe (estimated actual values in parentheses). [c] Estimated minimum solids residence time.

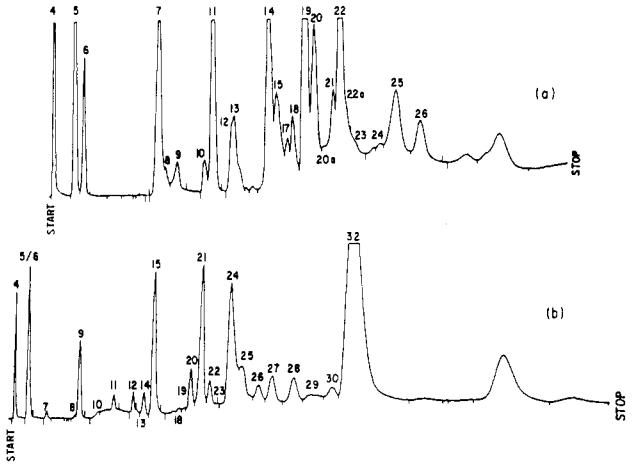

Figure 4. Chromatogram obtained for MCP pyrolyzed in a Pyroprobe 100 instrument (a) from a Porapak Q column (FID) (numbered peaks are identified in Table IV) and (b) from a Porapak T column (FID) (numbered peaks are identified in Table V).

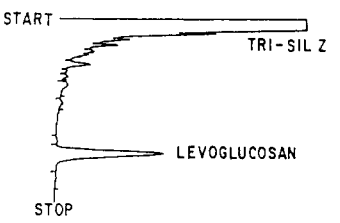

Figure 5. Chromatogram of a silylated tar sample using a OV-101 column.

channels used FID's, and temperature programming was employed. A second chromatograph equipped with a 1.8-m 80/100-mesh 5A molecular sieve column was used to measure CO and hydrogen.

Tar samples were treated with *N*-(trimethylsilyl)-imidazole in pyridine to volatilize levoglucosan. Silylated tar solution was injected onto a 1.8-m 6% OV-101 on 80/100-mesh Chromosorb column, and peaks were detected with an FID-equipped GC. A chromatograph of the silyated tar is shown in Figure 5. The small peaks between the silylation agent and levoglucosan were not identified.

Experimental Program

Materials Employed. A microcrystalline cellulose (MCP) furnished as a 200/270-mesh powder by Canlab (Toronto, Ontario) was the primary material studied. Cellulose particles, as a 20/40-mesh material, were made by pelletizing the MCP, crushing, and then sieving.

A second cellulose source, Whatman ashless filter paper No. 44, clipped into fine strips sized 5 × 1 × 0.2 mm was also used. Although this source could only be used in the Pyroprobe experiments because of feed difficulties, its use permitted a study of the effect of the type of cellulose on product yields. Particles and powder were used in both the Pyroprobe and the fluidized bed.

Variables Studied. Variables considered in this work are shown in Table III. The temperature range used in the fluidized beds was effectively determined by blockage of either the feed inlet or products outlet at high and low temperatures. For the Pyroprobe, both of the final temperatures indicated on the instrument and estimates of the actual temperatures from thermocouples located on the quartz boat or imbedded in the sample are shown. Nominal heating rates are shown in the table along with the estimated actual rates, but temperature rise is not linear with time throughout the entire heating process because of the endothermicity of pyrolysis. Heating rates in the fluidized bed could not be measured but are believed to be very rapid because of the dispersion of cellulose in the bed as fine particles.

Contact time in the fluidized bed could not be measured. The time given in Table III was estimated by assuming that the gas fed to the bed moves through the vessel in plug flow. It was kept constant in all experiments. Actual contact time could have been much greater. No unconverted cellulose was recovered in the condenser. Consequently, cellulose remains in the bed until it is fully pyrolyzed.

Correlation of Product Yields and Weight Loss

Product yields, defined as the weight of product collected divided by the weight of sample, were found to correlate the product distribution data well. Although temperature in the fluidized bed correlated the product yield satisfactorily, the correlation of yields with final pyrolyzer temperature was poor. This difference in behavior results from the considerable difference in behavior of the two pyrolyzers. In the fluidized bed, finely divided cellulose reaches the bed temperature very rapidly, probably requiring just a few milliseconds. Even in this situation, pyrolysis may not occur at constant temperature because, according to the model of Lewellen et al. (1977), consumption of 90% of the sample (by weight) requires only 0.18 ms at 1000 °C and 2.2 ms at 800 °C. Once products are formed, however, they leave the bed in a uniform temperature environment with an almost uniform residence time of about 0.5 s. In contrast, cellulose in the Pyroprobe experiments was exposed in small heaps or piles. Thermocouple measurements show heating rates well below those indicated on the instrument. Even at the highest heating rates, it took 1–2 s to reach the final py-

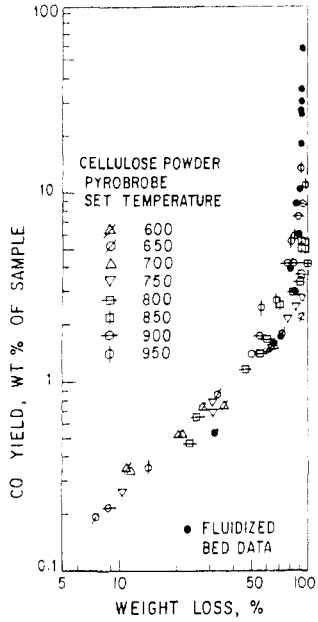

Figure 6. CO yield for pyrolysis of MCP in a Pyroprobe 100 and in the fluidized bed (Weight loss in the fluidized bed is 100 wt % char): ○ = MCP; ● = fluidized bed.

rolyzer temperature. Pyrolysis occurred entirely then under varying temperature. Furthermore, pyrolysis products in the sample diffuse first through the pyrolyzing material (against a strong thermal gradient) and emerge into a gas environment that could be changing in temperature depending on the heating rate and soaking times. The temperature environment for further cracking of the primary pyrolysis products, consequently, is quite different. Product cooling is much faster in the Pyroprobe than in the fluidized bed. Although this may not be a reason for the poor correlation of yields with temperature for the Pyroprobe, it may help to explain the lack of correspondence between yields from the fluidized bed and the Pyroprobe when plotted against the bed or final temperature.

Other researchers (Simmons and Sanchez, 1981; Kato 1967) have found that weight loss correlates product yields under flash pyrolysis conditions. Use of weight loss as the independent variable meant, unfortunately, that only the low bed temperature data (<500 °C) from the fluidized bed experiments could be used. At higher temperatures, weight loss was essentially 100%. Consequently, most of the data presented below were obtained by using the Pyroprobe.

At the end of the Pyroprobe experiments, the boat appeared to be tar-free. Deposits were found on the quartz tube holding the boat and on the heating coil. It was assumed, therefore, that the residue in the quartz boat was just unconverted sample and char. If char forms from condensation of reaction pyrolysis products, that is, through tar, it is likely that most of the residue is unconverted sample. In this case, weight loss should closely represent the weight percent of the sample pyrolyzed.

Figure 6 plots the carbon monoxide yield against weight loss also as a percent of sample for cellulose powder. Data for both the fluidized bed and the Pyroprobe are shown. The indicated heating rate for the latter was 20 °C/ms, but the heating rate was not found to influence the yield vs. weight loss relationship. Up to a 40–50% weight loss, there seems to be no influence of temperature (or soaking period). CO yield in this region is linear with weight loss on a logarithmic plot, so the relation is

$$\text{Product Yield} = A(\text{Co yield})^B \qquad (1)$$

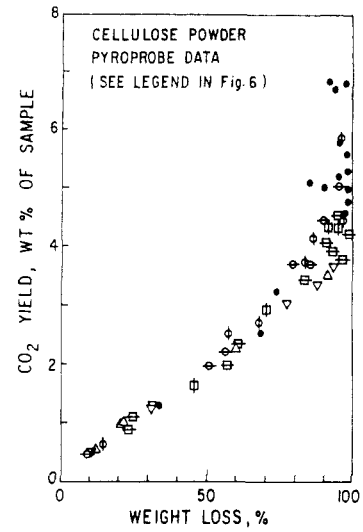

Figure 7. CO_2 yield for pyrolysis of MCP in the Pyroprobe and in the fluidized bed (symbols as in Figure 6).

Above about 60% weight loss, Y_{CO} becomes a function of the final temperature as well as weight loss. Possibly, eq 1 still applies but b, at least, becomes a function of temperature. Funazukuri (1983) finds that

$$Y_{CO} = 0.0096(2.5\Delta W)^{\alpha} \qquad (2)$$

describes the Pyroprobe results satisfactorily for $\Delta W > 0.04$. In this relation, both Y and ΔW are weight fractions. The exponent α is a logarithmic function of the reciprocal of the final pyrolyzer temperature in degrees kelvin.

For the fluidized bed data, CO yield varies almost linearly with the bed temperature: the uppermost point in the figure corresponds to 770 °C, while the lowermost to 310 °C. Because the Pyroprobe data points are given with indicated rather than actual temperatures, agreement between the points from the different instruments is poor. However, even correcting the Pyroprobe points to actual final temperatures as measured by separate thermocouple experiments does not produce exact agreement.

Figure 7 shows the yield of carbon dioxide as a function of weight loss. CO_2 yield is a linear function of weight loss up to 70% weight loss; thereafter, a slight temperature dependence appears. Nonetheless, the CO_2 data are rendered satisfactorily by

$$Y_{CO_2} = a'\Delta W \qquad (3)$$

up to $\Delta W = 100\%$.

There is excellent agreement of data from the two instruments except at close to 100% weight loss, where data from both experiments scatter.

Methane and acetaldehyde yields from the pyrolysis of MCP in a Pyroprobe are shown in Figure 8. For both products, yield appears to be linear with weight loss on a log–log plot and independent of final Pyroprobe temperature up to about 50% weight loss. Above this level, yields become strong functions of the final temperature. The yield vs. weight loss behavior for both products seems identical with that shown in Figure 6 for CO. Hydrocarbons up to C_5 were found in the gas products. The C_2, C_3, and C_4 fractions behave exactly as methane or CO with respect to yield vs. weight loss. Methanol, benzene, and crotonaldehyde yields also behaved as acetaldehyde or CO. Incomplete separation in the chromatograph for acrolein, furan, acetone, and the ketones (methyl ethyl and methyl vinyl) meant differences in peak areas had to be used to

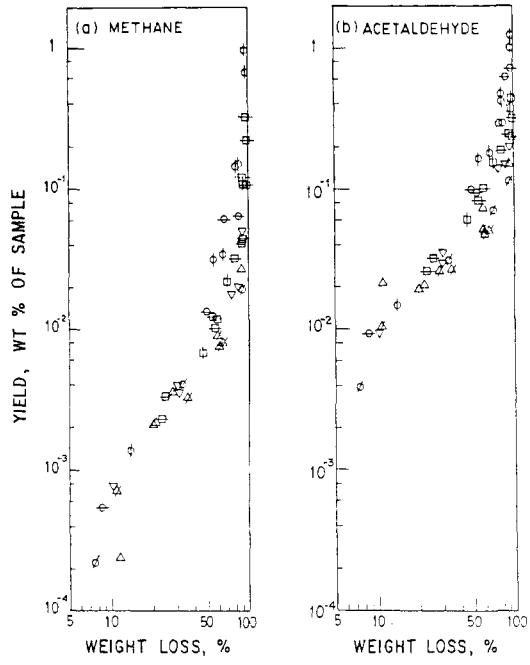

Figure 8. Yield for pyrolysis of MCP in a Pyroprobe: (a) methane, (b) acetaldehyde (symbols as in Figure 6).

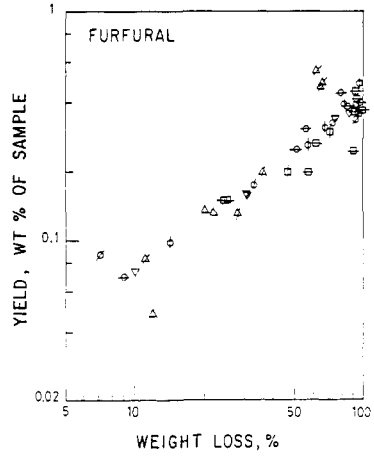

Figure 9. Furfural yield for pyrolysis of MCP in a Pyroprobe (symbols as in Figure 6).

calculate yields. Yields at low conversions were very small so the errors in these determinations were large. Nonetheless, if we disregard the badly scattered data at weight losses below 10–20%, the yield vs. weight loss behavior for these products also looks like Figure 8.

Figure 9 plots furfural yields for cellulose powder. The slope is fairly close to unity, and there is very little temperature dependence of yield even at high weight loss compared to the behavior seen in Figure 8. Furfural, thus, exhibits the same yield vs. weight loss behavior as CO_2. Yields for water, 2-methylfuran, butyric acid, and toluene also resemble the CO_2 behavior.

Levoglucosan is not stable at temperatures in the usual flash pyrolysis range. Thus, its behavior would not be expected to resemble either those shown for CO or CO_2. Figure 10 shows that levoglucosan yields go through a maximum with respect to weight loss. This maximum is indistinct in Figure 10 but seems to lie in the 60–90% weight loss range. The levoglucosan data are for both MCP and cellulose particles made from MCP. All measurements were made in a fluidized bed with a nitrogen carrier gas. Levoglucosan yields plot linearly vs. bed temperature, decreasing to almost zero at a bed temperature of 770 °C.

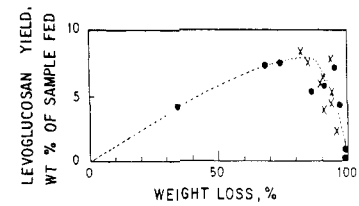

Figure 10. Levoglucosan yields for pyrolysis of MCP in a fluidized bed. ● = MCP; × = cellulose particles.

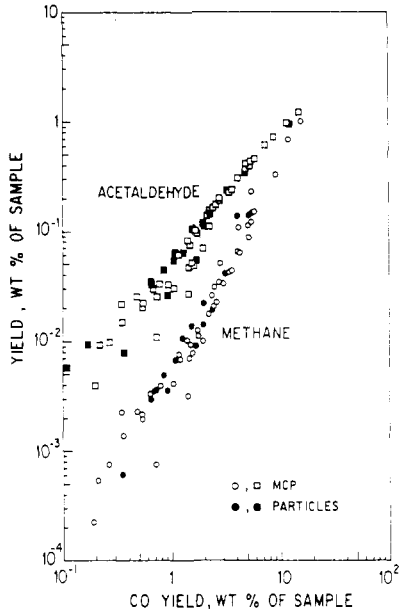

Figure 11. CH_4 and acetaldehyde yields for MCP and particles as a function of CO yield for pyrolysis: ○ = CH_4 from MCP; ● = CH_4 from cellulose particles; □ = acetaldehyde from MCP; ■ = acetaldehyde from cellulose particles.

Correlation of Product Yields with Carbon Oxide Yields

Correlation of Product Yields. The similarity of the yield vs. weight loss curves seen in Figure 6 and 8 and Figures 7 and 9 suggests correlating yields of the various products against one product. Since CO is the product with the largest yield in its group, it was chosen as the correlating variable. Figure 11 combines the data shown in Figures 6 and 8. The resulting cross plot of yields indicates a linear relationship between the logarithms of the methane and acetaldehyde and carbon monoxide yields for MCP and cellulose particles. The relationship, thus, has the form

$$Y_{\text{product}} = A(Y_{\text{CO}})^B \tag{4}$$

The coefficient and exponent are given in Table VI for methane, acetaldehyde, and other members of this behavior group. Final soaking temperature in the instrument does not influence the relationship. Particle size, also, is not important. The scatter at CO yields < 1 wt % probably reflects measurement uncertainty as well as some minor temperature effects at the low final temperatures used for these measurements.

Note that exponents of the logarithmic relations given in Table VI fall into ranges which correspond to product groups. Hydrocarbons, thus, all have exponents of about 2. Aldehydes, furan, and acetone have exponents of unity which indicate a linear relationship between yields of CO and yields of these products. Methanol, acrolein, and benzene have almost identifical exponents about midway between those of the two previous groups.

Table IV. Identification of Peaks Shown in the Chromatogram of Figure 4a (Porapak Q Column—Pyrolysis of Cellulose Powder in a Pyroprobe)

peak no.	component
4	methane
5	ethylene + acetylene
6	ethane
7	propylene
8	propane
9	cyclopropane
10	methanol
11	acetaldehyde
12	butene
13	butane
14	acrolein + furan
15	acetone + propionaldehyde
16	?
17	?
18	pentene + pentane
19	acetic acid + isobutyraldehyde + 2-methylpropenal(?)
20	2-methylfuran
20a	methyl ethyl ketone + methyl vinyl ketone
21	crotonaldehyde
22	benzene
22a	propionic acid
23	2,5-dimethylfuran
24	butyric acid
25	toluene
26	furfural

Table V. Identification of Peaks Shown in the Chromatogram of Figure 4b (Porapak T Column—Pyrolysis of Cellulose Powder in a Pyroprobe)

peak no.	component
4	methane
5	ethylene + ethane
6	?
7	acetylene
8	?
9	propylene + propane
10	cyclopropane
11	?
12	butene
13	butane
14	butadiene
15	methanol + acetaldehyde
16	?
17	?
18	pentene
19	pentene
20	furan
21	acrolein + propionaldehyde
22	acetone
23	?
24	2-methylfuran + isobutyraldehyde + 2-methylpropenal(?)
25	butyraldehyde
26	methyl ethyl ketone + methyl vinyl ketone
27	benzene
28	2,5-dimethylfuran + crotonaldehyde
29	?
30	?
31	?
32	toluene + acetic acid + ?

Yields of carbon dioxide are plotted vs. those of carbon monoxide in Figure 12. A linear relationship on logarithmic coordinates extends to about a CO yield of 3 wt %, where a slope change occurs. Up to this point, parameters of eq 4 for CO_2 may be found in Table VI. The table gives parameters as well for the products which exhibit CO_2 yield vs. weight loss behavior.

It might be expected that plotting yields of products behaving like CO_2 rather than CO against CO_2 yields would give linear relationships. This is indeed the case as Figure 13 shows. The figure is a cross plot of data from Figures 7 and 9. (Data for cellulose particles and filter paper are also shown. They will be discussed later.) The linear relation with logarithmic coordinates gives rise to

$$Y_{\text{product}} = A'(Y_{CO_2})^{B'} \quad (5)$$

where the parameters A' and B' are collected in Table VII. The exponent for furfural is close to unity so there is indeed a linear relationship between furfural and CO_2 yields. Table VII gives the parameters of eq 5 for the other products showing the CO_2 yield vs. weight loss behavior. With the exception of 2-methylfuran, the exponents B' are close to unity.

Table VI. Parameters of the Linear Fits to Logarithmic Plots of Product Yield vs. CO Yield[a]

$$\text{Product Yield} = A(\text{Co yield})^B \quad (1)$$

	A	B	effective max CO yield, wt % of sample
CH_4	4.25×10^{-3}	2.0	15
$C_2H_4 + C_2H_6$	8.19×10^{-3}	1.85	15
$C_3H_6 + C_3H_8$	5.13×10^{-3}	1.83	15
$C_4H_8 + C_4H_{10}$	1.90×10^{-3}	2.00	15
methanol	6.18×10^{-3}	1.58	15
acetaldehyde	5.61×10^{-2}	1.15	15
acrolein	2.74×10^{-2}	1.58	10
crotonaldehyde	4.32×10^{-2}	0.99	10
furan	2.56×10^{-2}	0.80	14
acetone	1.80×10^{-2}	1.08	14
benzene	7.13×10^{-3}	1.63	10
CO_2	1.43	0.76	3
water	3.91	0.90	3
butyric acid	9.00×10^{-2}	0.92	2
2-methylfuran	9.85×10^{-2}	1.15	2
toluene	2.12×10^{-1}	1.07	2
furfural	1.72×10^{-1}	0.70	3

[a] Note: CO yield [wt % of sample]; product yield [wt % of sample].

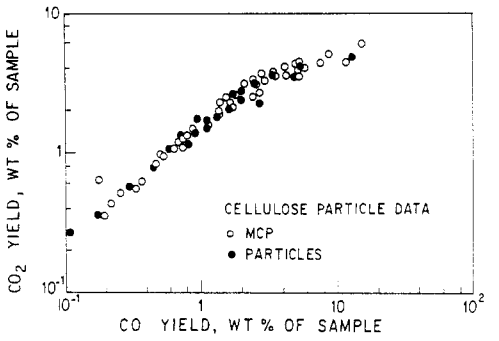

Figure 12. CO_2 yield as a function of CO yields for MCP and cellulose particles for pyrolysis: o = MCP; ● = cellulose particles.

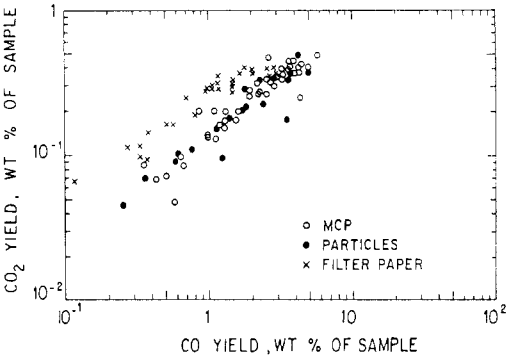

Figure 13. Furfural yield as function of CO_2 yield for MCP, cellulose particles, and filter paper (symbols as in Figure 12 with × = filter paper).

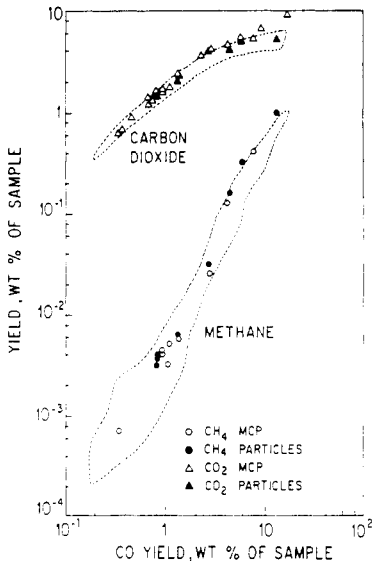

Figure 14. Effect of heating rate on the CH_4 and CO_2 yield correlations with CO (Pyroprobe data); area enclosed by dashed line = CH_4 and CO_2 yields from MCP at 20 °C/ms nominal heating rate. Data points are for nominal heating rate of 0.1 °C/ms for both MCP and cellulose particles.

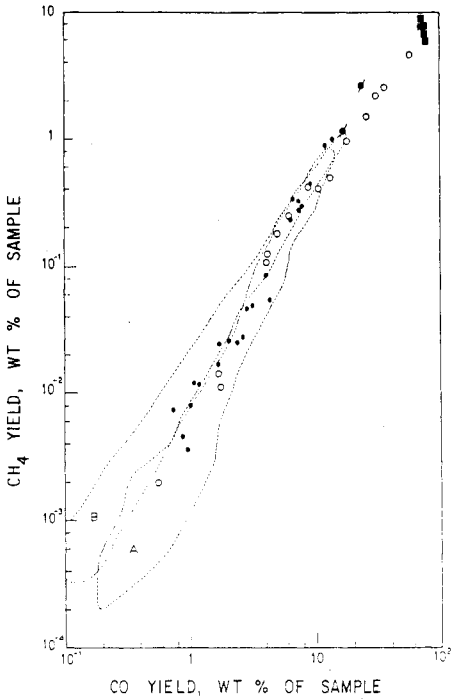

Figure 15. Effect of pyrolysis device and type of cellulose on CH_4 yield correlation; dashed enclosed are A = MCP pyrolysis in the Pyroprobe; dashed enclosed area B = filter paper in the Pyroprobe; ○ = MCP in the fluidized bed. Solid symbols are values from the literature: ● = Martin (1965); ◖ = Hajaligol et al. (1982); ■ = Graham et al. (1982).

Influence of Experimental Variables. Cellulose particle size has no effect on the product yield correlation. Data points for MCP and particles made from powder intermingle on Figures 11–13 even though there is more than an order of magnitude difference in particle size between the materials.

Figure 14 examines the influence of heating rate on the methane and CO_2 yield relationships. Data for the nominal heating rate of 0.1 °C/ms (actual rate about 0.035 °C/ms) are superimposed on the data regions for a nominal heating rate of 20 °C/ms (actual rate about 0.3 °C/ms). Data for both MCP and particles are shown. Thus, cross plotting of product yields vs. CO yields eliminates any influence of heating rate even though a 10-fold change in the actual heating rate exists. In Figures 6 and 7, both Pyroprobe

Table VII. Parameters of the Linear Fits to Logarithmic Plots of Product Yield vs. CO_2 Yield[a]

Product Yield = $A'(CO_2 \text{ yield})^{B'}$

	A'	B'	effective max CO yield, wt % of sample
2-methylfuran	5.75×10^{-2}	1.43	6
butyric acid	4.51×10^{-2}	1.28	5
furfural	1.33×10^{-1}	0.80	6
toluene	1.15×10^{-1}	1.22	3

[a] Note: product yield [wt % of sample], CO_2 yield [wt % of sample].

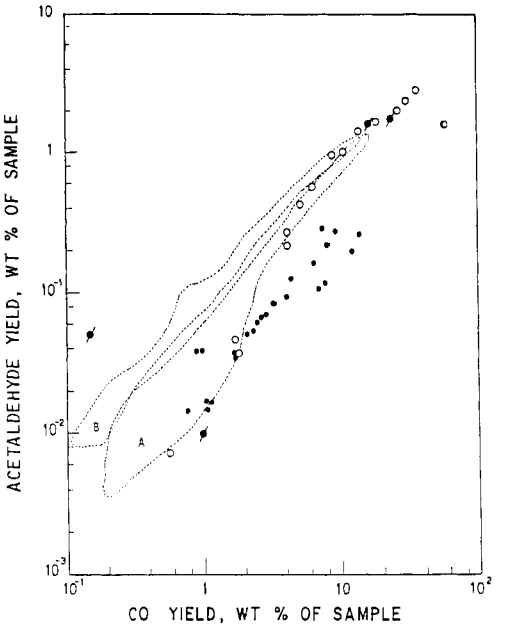

Figure 16. Effect of pyrolysis device and type of cellulose on acetaldehyde yield correlation: dashed enclosed area A = MCP in the Pyroprobe; dashed enclosed area B = filter paper in the Pyroprobe; ○ = MCP in the fluidized bed. Solid symbols are values from the literature: ● = Martin (1965); ◖ = Hajaligol et al. (1982).

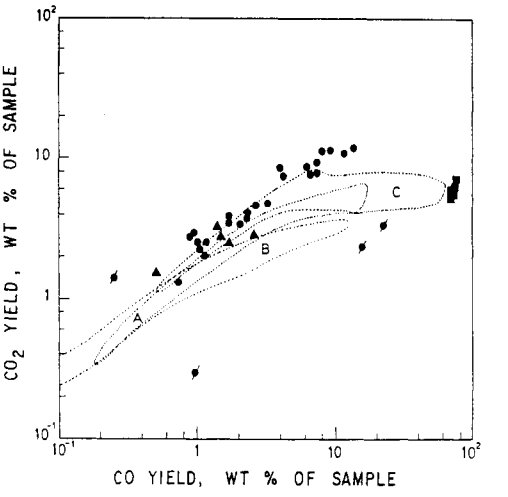

Figure 17. Effect of pyrolysis device and type of cellulose on CO_2 yield correlation: dashed enclosed area A = CO_2 yields from MCP in the Pyroprobe; dashed enclosed area B = CO_2 yields from filter paper in the Pyroprobe; C = CO_2 yields from MCP in the fluidized bed. Solid symbols are values from the literature: ● = Martin (1965); ■ = Graham et al. (1982); ◖ = Hajaligol et al. (1982); ▲ = Tsuchiya and Sumi (1970).

and the fluidized bed are shown. The data seem to form a single population. Figures 15–17 examine the effect of pyrolysis device more explicitly. Methane yield data for MCP in a fluidized bed pyrolyzer plotted in Figure 15 agree closely with the data gathered in the Pyroprobe unit. Close agreement is also seen in Figure 16 which plots acetaldehyde yields. For CO_2, the fluidized bed data which includes both MCP and cellulose particle measurements lie somewhat above the Pyroprobe data region. Thus, differences, if any, are small, and it seems reasonable to conclude that product vs. CO yield relationships are not dependent on the type of pyrolyzing equipment.

Type and/or molecular weight of cellulose seem to be the only variables which influence the yield relationships among those examined. Pyrolysis of finely cut filter paper was carried out by using the Pyroprobe 100 unit. The filter paper was lignin- and hemicellulose-free, essentially zero-ash, long-fiber cellulose. The cellulose molecular weight was much greater than in MCP. Methane vs. CO yields for filter paper are shown as a data region in Figure 15. The same comparison is given in Figure 16 for acetaldehyde. For both products, yields obtained from filter paper are higher than yields from the lower molecular weight and crystalline MCP at the same CO yield. Furfural yields from these materials are compared in Figure 13. Again, yields of furfural are above those for MCP and particles at the same CO_2 yield. For CO_2, however, the relation of MCP and filter paper is reversed. As may be seen from Figure 17, at low CO yield or low weight loss, the filter paper and MCP data overlap, but at higher CO yields, the CO_2 yield for filter paper is less than the yield for MCP.

Even though differences can be seen depending on the cellulose used, Figures 15 and 16 demostrate that a relationship of the form of eq 4 applies to yields from filter paper. The parameters of the relationship depend on the material.

Results of Other Investigators. Figures 15–17 show the yield measurements of other authors cross-plotted as in Figures 11 and 12. Martin (1965) used a α-cellulose sheet in an air atmosphere. The material would be expected to behave much as filter paper. Tsuchiya and Sumi (1970) used filter paper in vacuum as did Hajaligol et al. (1982). The latter authors worked in helium at subatmospheric pressure. Graham et al. (1982) employed MCP with helium at atmospheric pressure. The experiments were also briefly described in the introductory section. With the exception of Tsuchiya and Sumi, the studies employed flash pyrolysis conditions. The CH_4 vs. CO yield relationship given by the data of Graham et al. (1982) for MCP seems to form an extension of the data obtained in this work. Placing MCP in the sheet form, which was the material used by Martin (1965), results in data which overlap those taken in this work. Even the filter paper results in Hajaligol et al. (1982) show general agreement with the data in the B region in Figure 15. The results obtained for acetaldehyde by Martin and Hajaligol et al., shown in Figure 16, show poorer agreement. The Martin data are well below the MCP data in the Figure. The data of Hajaligol et al. scatter badly.

Data of all investigating groups are shown in Figure 17. Results of Graham et al. with MCP again seem to be an extension of the data obtained in this work. The filter paper data of Hajaligol et al. for CO_2 scatter badly and fail to agree with any of our data. Martin's results fall above our MCP data. Despite the disagreement of particular sets of data, the large measure of agreement supports the accuracy of the measurements made in this study.

Interpretation

Even though this study was not designed to elucidate pyrolysis mechanisms, the striking cross-correlations discussed in the previous sections may provide some insight into the pyrolysis process. According to Shafizadeh (1982), pyrolysis proceeds between 300 and 500 °C by depolymerization of cellulose to anhydroglucose units followed by conformation changes such as transglycosylation to yield levoglucosan as the major product. Levoglucosan is not stable and disproportionates. Above 500 °C, fission of levoglucosan occurs along with dehydration and decarboxylation. Primary products of levoglucosan pyrolysis are formaldehyde, furfural, acetaldehyde, higher aldehydes, diacetyls, water, CO_2, and CO. Measurements in this study of furans, acetaldehyde, and furfural which arise through depolymerization and levoglucosan cracking indicate that these steps must also occur under very fast heating. Carbon dioxide also arises in the above sequence so that perhaps the products which correlate well with CO_2 yield are largely formed through the depolymerization–levoglucosan cracking route. Yields through this route would be expected to depend only on the cellulose decomposed, e.g., weight loss.

Demonstrating similar products for flash pyrolysis of various organic materials at temperatures above 700 °C, Diebold (1980) suggests that random scission of the cellulose molecule must occur, generating free radicals such as HOC(H):, H·, HOC(H_2):, HC:, HOC:, etc. These radicals rapidly recombine to form alcohols, aldehydes, alkenes, alkanes, and aromatics as well as H_2, CO, and H_2O. The occurrence of benzene, methanol, and alkanes at low CO yields or low pyrolysis temperatures indicates that random scission of cellulose and free-radical reactions must be occurring at temperatures below 500 °C.

Radical formation is strongly temperature-dependent. Thus, it seems likely that those products whose yields are functions of weight loss and pyrolysis temperature, such as CO, form primarily through the random scission/free-radical mechanism. The observations of this study are adequately explained by postulating that pyrolysis proceeds through the two parallel routes just described. As the pyrolysis temperature increases, the random scission-free radical route becomes dominant.

Acknowledgment

An educational grant from C-I-L Inc. that made this project possible is gratefully acknowledged. Dr. D. S. Scott kindly made available the microfluidized bed and the extensive facilities of his pyrolysis laboratory. We are grateful for his expert advice and that of his associate, J. Piskorz.

Registry No. CO, 630-08-0; CO_2, 124-38-9; cellulose, 9004-34-6; methane, 74-82-8; ethylene, 74-85-1; acetylene, 74-86-2; ethane, 74-84-0; propylene, 115-07-1; propane, 74-98-6; cyclopropane, 75-19-4; methanol, 67-56-1; acetaldehyde, 75-07-0; butene, 25167-67-3; butane, 106-97-8; acrolein, 107-02-8; furan, 110-00-9; acetone, 67-64-1; propionaldehyde, 123-38-6; pentene, 25377-72-4; pentane, 109-66-0; acetic acid, 64-19-7; isobutyraldehyde, 78-84-2; 2-methylfuran, 534-22-5; methyl ethyl ketone, 78-93-3; methyl vinyl ketone, 78-94-4; crotonaldehyde, 4170-30-3; benzene, 71-43-2; propionic acid, 79-09-4; 2,5-dimethylfuran, 625-86-5; butyric acid, 107-92-6; toluene, 108-88-3; furfural, 98-01-1; butadiene, 106-99-0; butyraldehyde, 123-72-8.

Literature Cited

Antal, M. J.; Friedman, H. L.; Rogers, F. E. *Combust. Sci. Technol.* **1980**, *21*, 141.
Barooah, J. N.; Long, V. D. *Fuel* **1976**, *55*, 116.
Berkowitz-Mattuck, J. B.; Noguchi, T. *J. Appl. Polym. Sci.* **1963**, *7*, 709.
Broido, A. *Pyrodynamics* **1966**, *4*, 243.
Broido, A.; Evett, M.; Hodges, C. C. *Carbohydr. Res.* **1975**, *44*, 267.
Brunner, P. H.; Roberts, P. V. *Carbon* **1980**, *18*, 217.

Byrne, G. A.; Gardiner, D.; Holmes, F. H. *J. Appl. Chem.* **1966**, *16*, 81.
Diebold, J. P. "Thermal Conversion of Solid Wastes and Biomass", American Chemical Society: Washington, DC, 1980; ACS Symp. Ser. No. 130, p 209-226.
Fairbridge, C.; Ross R. A.; Sood, S. P. *J. Appl. Polym. Sci.* **1978**, *22*, 497.
Funazukuri, T. Ph.D. Dissertation, University of Waterloo, Waterloo, Ontario, Canada, 1983.
Garn, P. D.; Denson, C. L. *Text. Res. J.* **1977a**, *47*, 485.
Garn, P. D.; Denson, C. L. *Text. Res. J.* **1977b**, *47*, 535.
Garn, P. D.; Denson, C. L. *Text. Res. J.* **1977c**, *47*, 591.
Glassner, S.; Pierce, A. R. *Anal. Chem.* **1965**, *37*, 525.
Graham, R.; Bergougnou, M. A.; Mok, L. K.; de Lasa, H. L. Research Paper Presented at "Fundamentals of Thermochemical Biomass Conversion": An International Conference, Estes Park, CO, Oct 1982.
Hajaligol, M. R.; Howard, J. B.; Longwell, J. P.; Peters, W. A. *Ind. Eng. Chem. Process Des. Dev.* **1982**, *21*, 457.
Hileman, F. D.; Wojcik, L. H.; Futrell J. H.; Einhorn, I. N. "Thermal Uses and Properties of Carbohydrates and Lignins"; Shafizadeh, F., Sarkanen, K., Tillman, D. A., Eds.; Academic Press: New York, 1976; pp 49-71.
Iglauer, N.; Bentley, F. F. *J. Chromatogr. Sci.* **1974**, *12*, 23.
Kaiser, E. R.; Friedman, S. B. *Combustion* **1968**, May, 31.
Kato, K. *Agric. Biol. Chem.* **1967**, *31*, 657-663.
Kato, K.; Takahashi, N. *Agric. Biol. Chem.* **1967**, *31*, 519.
Kato, K.; Komorita, H. *Agric. Biol. Chem.* **1968**, *32*, 21.
Lewellen, P. C.; Peter, W. A.; Howard, J. B. Proceedings of the 16th International Symposium on Combustion, Pittsburgh, PA, 1977, p 1471.
Maa, P. S.; Baille, R. C. 84th National Meeting of The American Institute of Chemical Engineering, Atlanta, GA, Feb 1978.
Martin, S. Proceedings of the 10th International Symposium on Combustion, Pittsburgh, PA, 1965, p 877.
Min, K. *Combust. Flame* **1977**, *30*, 285.
Ohnishi, A.; Kato, K.; Takagi, E. *Polym. J.* **1975**, 431.
Rensfelt, E.; Blomkvist, G.; Ekstrom, C.; Engstrom, S.; Espenas, B.-G.; Liinanki, L. Proceedings of the Symposium on Energy from Biomass and Wastes, Washington, DC 1978.
Sakuma, H.; Munakata, S.; Sugawara, S. *Agric. Biol. Chem.* **1981**, *45*, 443.
Scott, D. S.; Piskorz, J. Final Contract Report, Waterloo Research Institute, Waterloo, Ontario, Canada, 1981a.
Scott, D. S.; Piskorz, J. "Fuels From Biomass and Wastes"; Klass, D. L., Emert, G. H., Eds.; Ann Arbor Science: Ann Arbor, MI, 1981b.
Schwenker, R. F.; Beck, L. R. *J. Polym. Sci., Part C* **1963**, 331.
Shafizadeh, F. *Adv. Carbohydr. Chem.* **1968**, *23*, 419.
Shafizadeh, F.; Bradbury, A. G. W. *J. Appl. Polym. Sci.* **1979**, *23*, 1431.
Shafizadeh, F.; Fu, Y. L. *Carbohydr. Res.* **1973**, *29*, 113.
Shafizadeh, F.; Furneaux, R. H.; Stevenson, T. T.; Cochran, T. G. *Carbohydr. Res.* **1978**, 433.
Shafizadeh, F.; Furneaux, R. H.; Cochran, T. G.; Scholl, J. P.; Sakai, Y. *J. Appl. Polym. Sci.* **1979a**, *23*, 3525.
Shafizadeh, F.; Furneaux, R. H.; Stevenson, T. T. *Carbohydr. Res.* **1979b**, *71*, 169.
Shafizadeh, F. *J. Anal. Appl. Pyrolysis* **1982**, *3*, 283.
Shivadev, U. V.; Emmons, H. W. *Combust. Flame* **1974**, *22*, 223.
Simmons, G.; Sanchez, M. *J. Anal. Appl. Pyrolysis* **1981**, *3*, 161.
Tsuchiya, Y.; Sumi, K. *J. Appl. Polym. Sci.* **1970**, *14*, 2003.
Wodley, F. A. *J. Appl. Polym. Sci.* **1971**, *15*, 835.

Received for review August 1, 1984
Revised manuscript received May 7, 1985
Accepted May 20, 1985

Longitudinal Mixing of the Liquid Phase on a Cocurrent Valve Tray with Entrainment Separators

Zhivko Tassev,* Zhelcho Stefanov, and Dimitar Kamenski

Chemical Engineering Department, Higher School of Chemical Technology, 8010 Bourgas, Bulgaria

Experimental data on liquid-phase mixing on a novel valve tray (cocurrent valve tray with entrainment separators) were obtained by the impulse method. The study was carried out in a rectangular column section (0.28 × 1.0 m) and the air–water system. The liquid-phase longitudinal mixing coefficient was found to vary with the superficial gas velocity and the liquid flow rate per unit weir width, being 1.5–2 times less than that of the same construction without entrainment separators. The longitudinal mixing coefficient was shown to correlate with the superficial gas velocity and liquid flow rate per unit weir width with a maximum deviation less than ±10%.

The status of liquid mixing on a tray is an important factor influencing the plate efficiency. The intensity of longitudinal mixing is usually characterized by the coefficient D_L which depends on the tray type, the gas and liquid flow rates, and the separation between the phases. So far, the coefficients of longitudinal mixing in the liquid phase were estimated experimentally. This paper is aimed at estimating the degree of liquid mixing on a cocurrent valve tray with entrainment separators, enabling thus the estimating of the effect of backmixing in tray efficiency. The cocurrent valve tray (Aleksandrov et al., 1965) has found wide industrial application in plate columns, particularly at high liquid flow. It is a modified construction of the "Glitsch" valve plate, its distinguishing characteristic being that one leg is shorter than the other two. Simultaneously, the gas phase runs out at angles toward the plate and adds additional velocity component to the liquid. In this way, the cocurrent motion of the two phases over the tray increases admissible liquid flow rate. It may also be expected that the one-way motion of the two phases over the tray will result in a decrease in the cumulative effect of the stagnant zones which is characteristic of large diameter trays in a cross-current regime such as those reported by Porter et al. (1972) and Bell (1972). At higher liquid and gas flow rates, however, the liquid from the tray deposits over the downcomer and the plate efficiency decreases due to the worse separation between the phases. The previous studies (Tassev and Stefanov, 1982) have shown that the installation of suitable entrainment separators results in a considerable decrease in the entrainment of the cocurrent valve tray for a wide velocity range.

Method

The dispersion model developed by Danckwerts (1953), Taylor (1953), and Tichacek et al. (1957) is frequently applied to describe the longitudinal mixing in the liquid phase on a column tray. The cocurrent valve plate with entrainment separators operates on a cross-cocurrent scheme: the cross-current regime prevails at low flow rates of the gas phase, whereas at higher rates the regime is essentially cocurrent when the valves are fully open at the same slope to the direction of liquid flow. The presence of the entrainment separators improves the separation of the phases without changing the flow direction of the liquid. We have decided for the longitudinal dispersion model because, as we assume, there exists a uniform tur-

0196-4305/86/1125-0181$01.50/0